

## Technical notes

# Visual observations of supersonic transverse jets

D. Papamoschou, D. G. Hubbard

Dept. of Mechanical and Aerospace Engineering, University of California, Irvine, CA 92717, USA

Received: 1 July 1992/Accepted: 21 December 1992

**Abstract.** We present experimental results on penetration of round sonic and supersonic jets normal to a supersonic cross flow. It is found that penetration is strongly dependent on momentum ratio, weakly dependent on free-stream Mach number, and practically independent of jet Mach number, pressure ratio, and density ratio. The overall scaling of penetration is not very different from that established for subsonic jets. The flow is very unsteady, with propagating pressure waves seen emanating from the orifice of helium jets.

## 1 Introduction

The problem of supersonic injection into a supersonic cross flow has important applications in thrust vectoring of spacecraft and fuel injection in supersonic-combustion ramjet (SRAMJET) engines. While there has been considerable experimental and theoretical work in the past, a host of questions remain to be addressed. Central among them is how the relevant flow parameters independently affect penetration, and how the behavior of so-called “pressure matched” jets differs from that of underexpanded jets.

Fig. 1 depicts a simplified view of the jet flow, highlighting the essential features. Strong injection into a supersonic cross flow generates a bow shock wave, an inseparable and crucial feature of the flow field. The sketch of Fig. 1 represents a “pressure-matched” jet devoid of shock/expansion waves around its orifice. The majority of experiments in the literature encompass under-expanded jets, with the jet static pressure substantially higher than the static pressure of the cross flow in the vicinity of the jet orifice. In the experiments of Zukoski and Spaid (1964), gas was injected through a sonic orifice into a supersonic cross flow. It was shown that the penetration distance scaled with the ratio of jet to free-stream total pressures. Schetz et al. (1968) studied experimentally supersonic under-expanded transverse jets, and noted that penetration increases slightly with jet Mach number. The works by Schetz and Billig (1966) and by Billig et al. (1971) incorporate experimental data into more advanced models of the flow field and generate the important concept of the “effective back pressure”. McDaniel and Graves (1988) used laser-induced fluorescence to study penetration and

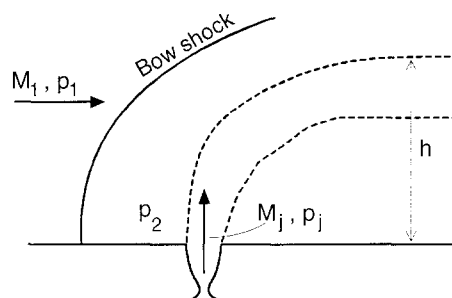


Fig. 1. Conceptual view of transverse jet

spreading of sonic under-expanded jets with low momentum ratio, and inferred a linear dependence of penetration on momentum ratio. Recently, Heister and Karagozian (1990) modeled the pressure-matched jet by means of a compressible vortex pair and obtained theoretical predictions of jet trajectory.

In the studies of Schetz and Billig and of Heister and Karagozian, it is pointed out that the pressure-matched jet is likely to achieve better penetration than the under-expanded jet. The reason is that under-expansion (as well as over-expansion) generates shock waves in the jet flow leading to creation of a Mach disk, which renders the jet flow subsonic. Surprisingly, there appear to be no systematic experimental comparisons of pressure-matched versus under-expanded transverse jets. Moreover, there is little experimental information on the effect of Mach numbers, uncoupled from the effects of other parameters. The goal of our study was to address these issues by covering both pressure-matched and under-expanded cases and attempting to isolate the role of each relevant flow variable.

## 2 Approach

It is known that penetration of the subsonic jet injected perpendicular to a subsonic free stream scales with the jet-to-cross flow momentum ratio,  $J = \rho_j U_j^2 / \rho_1 U_1^2$  (Abramovich 1963; Broadwell and Breidenthal 1984). In the supersonic case, the following additional variables are likely to

play a role: cross-flow Mach number  $M_1$ ; jet Mach number  $M_j$ ; pressure ratio at the jet exit,  $p_j/p_2$ ; density ratio at the exit,  $\rho_j/\rho_2$ . A parametric statement including the aforementioned parameters is

$$\frac{h}{d} = \frac{h}{d} \left( J, M_1, M_j, \frac{p_j}{p_2}, \frac{\rho_j}{\rho_2} \right) \quad (1)$$

where  $h/d$  is the penetration distance scaled by the jet-exit diameter. It is important to establish the interdependence of certain variables in Eq. 1. For compressible flow, the momentum ratio  $J$  can be written as

$$J = \frac{\gamma_j p_j M_j^2}{\gamma_1 p_1 M_1^2} \quad (2)$$

The normal-shock relation between  $p_2$  and  $p_1$

$$p_2 = p_1 \frac{2\gamma_1 M_1^2 - (\gamma_1 - 1)}{\gamma_1 + 1} \quad (3)$$

which for  $M_1 \geq 2$  is well approximated by

$$p_2 \approx p_1 \frac{2\gamma_1 M_1^2}{\gamma_1 + 1} \quad (4)$$

This enables us to relate  $J$  to  $p_2$  and write Eq. 1 in the form

$$\frac{h}{d} = \frac{h}{d} \left( J \approx \frac{2\gamma_j}{\gamma_1 + 1} \frac{p_j}{p_2} M_j^2, M_1, M_j, \frac{p_j}{p_2}, \frac{\rho_j}{\rho_2} \right) \quad (5)$$

It is evident that, for given  $p_j/p_2$ , the momentum ratio  $J$  is very strong function of  $M_j$ . For fixed  $J$ , one has no choice but to decrease  $p_j/p_2$  while increasing  $M_j$ , and vice-versa. This makes it difficult to distinguish between the individual effects of  $p_j/p_2$  and  $M_j$ . Eq. 5 shows that the cross-flow Mach number  $M_1$  has very weak influence on  $J$ , therefore  $M_1$  can be varied by a large extent while keeping all other variables virtually fixed. The same applies to density ratio, since  $J$  in the formulation of Eq. 2 is independent of molecular weight.

As noted earlier, it was desired to focus our study on “pressure-matched” jets. However, due to compressibility in the cross flow, the static pressure around the jet varies greatly along its circumference as well as along its trajectory, so it is difficult to define pressure matching. The computations of Heister and Karagozian (1990) showed that the “equivalent pressure” (the static pressure averaged around the jet perimeter) is approximately  $0.5 p_2$  for the range of  $M_1$ 's considered here. We will assume here that  $p_j = 0.5 p_2$  represents a “pressure-matched” condition, keeping in mind that there is some arbitrariness in selecting that value.

### 3 Facility and experimental conditions

Experiments were conducted in a blow-down supersonic wind tunnel at University of California, Irvine, depicted schematically in Fig. 2. The main flow consisted of air while the jet flow was supplied from pressurized helium and argon cylinders. The test-section Mach number took the values

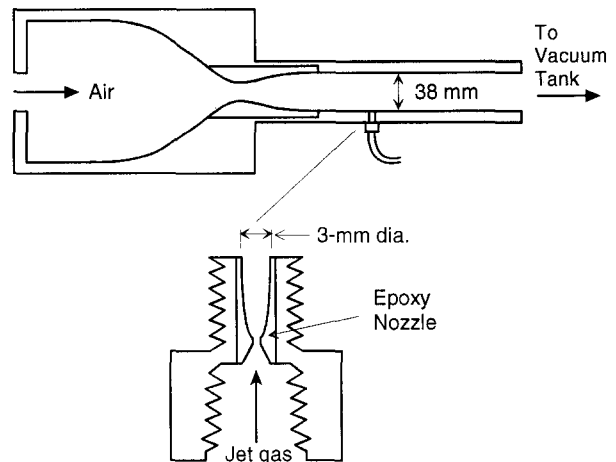


Fig. 2. Schematic of supersonic tunnel and jet module

$M_1 = 2$  and  $M_1 = 3$ . The test section is 38 mm high 64 mm wide and 500 mm long. Test-section static pressures were around 40 kPa for  $M_1 = 2$  and 20 kPa for  $M_1 = 3$ . Unit Reynolds numbers were in the neighborhood of  $45,000 \text{ mm}^{-1}$ . Replaceable modules, mounted flush with the test section wall, incorporate small supersonic nozzles for the transverse jet, each module for a different Mach number. The nozzles have smooth converging-diverging shapes formed by inserting a needle-shaped mold in wet epoxy and retracting it after the epoxy dried. Each mold had the desired shape and area ratio for a given jet Mach number. The nozzle diameter at the exit is  $d = 3 \text{ mm}$ . Modules were built for Mach numbers 1, 2.1, 2.8, and 3.5, corresponding to  $\gamma = 5/3$ .

The schlieren system has a focal length of 1 m and beam diameter of 150 mm. The light source is a 20-nanosecond spark gap (Xenon, Model 787-B). A horizontal knife edge was used for intercepting the light beam, accentuating gradients in the transverse direction. Images were captured by a CCD camera with  $576 \times 384$  pixel resolution (Photometrics Star I).

Table 1 lists the test cases and related conditions, tabulated in order of increasing momentum ratio  $J$ . Cases with the same first digit have the same value of  $J$ . The cross-flow gas in air for all cases.

### 4 Results

Representative schlieren pictures of the flow field are shown in Fig. 3, showing the helium cases 7a, 7b, and 7c and the argon case 7d. All four cases have  $J = 8.3$  and  $M_1 = 2$ , but the jet Mach number  $M_j$  is variable. Little difference is seen in the jet trajectory as  $M_j$  increases from 2.1 to 2.8 to 3.5. In terms of pressure ratio, the corresponding trend is from highly under-expanded to nearly pressure-matched. Also, the switch from helium to argon jet does not noticeably alter the jet trajectory.

**Table 1.** Transverse jet parameters

Case	$J$	$M_1$	$M_j$	$p_j/p_2$	$\rho_j/\rho_2$	Jet Gas
1a	1.7	2.0	1.0	1.3	0.22	He
1b	1.7	2.0	2.1	0.3	0.10	He
1c	1.7	3.0	2.1	0.3	0.10	He
2	2.4	2.0	2.8	0.2	0.14	He
3a	3.0	2.0	1.0	2.2	0.44	He
3b	3.0	2.0	2.1	0.5	0.18	He
3c	3.0	3.0	2.1	0.5	0.44	He
3d	3.0	3.0	2.8	0.3	0.14	He
4	4.2	2.0	3.5	0.3	0.20	He
5a	5.3	2.0	1.0	4.0	0.93	He
5b	5.3	2.0	2.1	0.9	0.29	He
5c	5.3	2.0	2.8	0.5	0.25	He
5d	5.3	3.0	2.8	0.5	0.24	He
6	6.6	3.0	4.3	0.3	0.27	He
7a	8.3	2.0	2.1	1.4	0.55	He
7b	8.3	2.0	2.8	0.8	0.40	He
7c	8.3	2.0	3.5	0.5	0.36	He
7d	8.3	2.0	3.5	0.5	3.60	Ar

As expected, the bow shock in front of the jet dominates the flow field. In the helium jets, the shock is wrinkled due to interaction with pressure waves emanating from the jet exit, probably caused by the turbulent eddies of the jet moving at supersonic speeds (around 1500 m/s) with respect to the surrounding air. In contrast, the argon jets are devoid of such waves and the bow shock is smooth. The eddies in the argon jet are subsonic with respect to the surrounding air, so they do not generate large pressure disturbances.

By comparing a large number of instantaneous pictures of the same flow field, we noticed that the shock structure is very unsteady. For example, the point of reflection of the shock with the upper wall moved as much as 10 mm (1/4 of test-section height) from one picture to the other. Unsteadiness appears to be a major aspect of this flow, something that computational models need to take into consideration. We were able to observe the turbulent structure of the jet for up to  $x/d \approx 20$ . The structure appears to have regular, repeating features, reminiscent of those seen in subsonic transverse jets.

The penetration height  $h$  is defined here as the maximum height of the jet trajectory, based on schlieren visualization of the upper edge of the jet. The trajectory is seen to level off at  $x/d \approx 6$ , which is where penetration measurements are referenced. Each value of  $h/d$  reflects an average of typically 5 individual trajectory heights measured from separate runs at the same condition. The error in  $h/d$  is estimated at 10%, based on the uncertainty of detecting the edge of the jet.

As already inferred from Fig. 3, our penetration measurements showed that, at fixed  $J$ ,  $M_1$  and  $M_j$ , the density ratio  $\rho_2/\rho_1$  does not influence penetration. Furthermore, penetration at fixed  $J$  and  $M_1$  is insensitive to  $M_j$ ; Fig. 4 depicts jet trajectories for cases, 7a–c, where no noticeable change occurs with increasing  $M_j$ . This also means that penetration is insensitive to the pressure ratio  $p_j/p_2$ , i.e., under-expanded

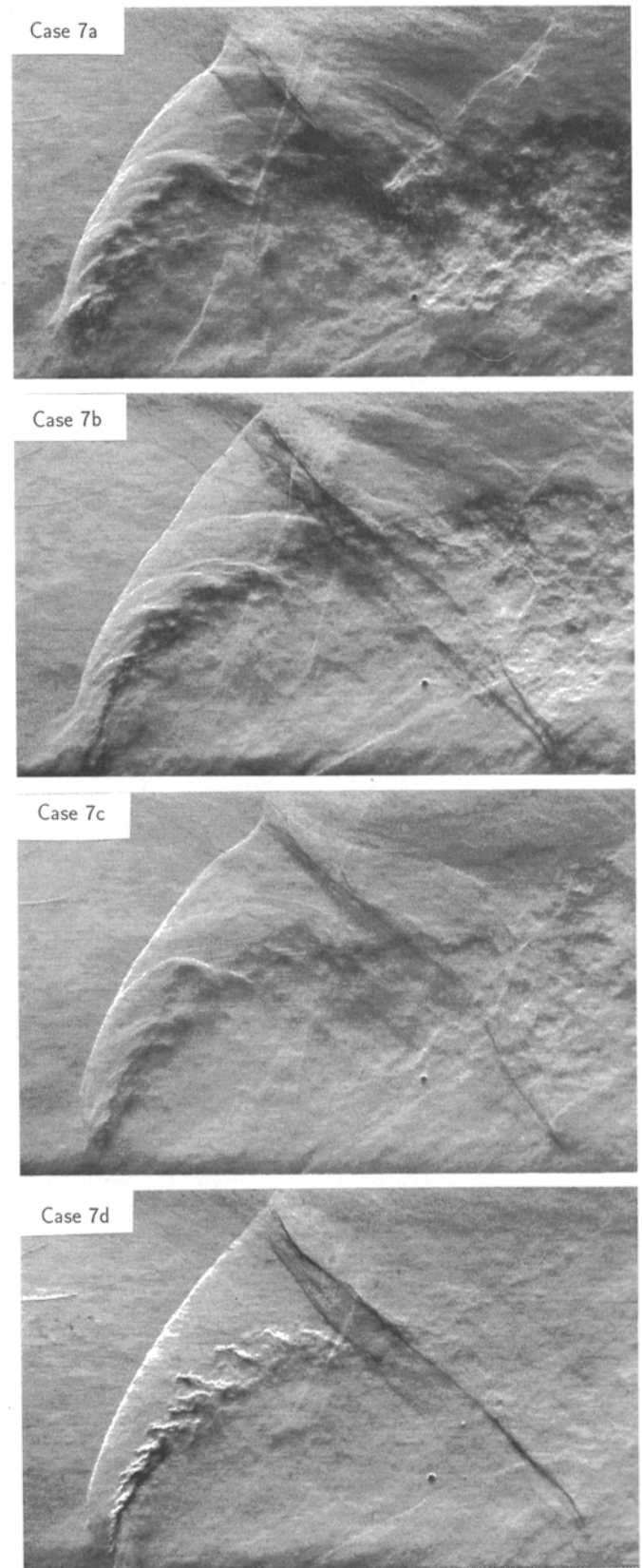


**Fig. 3.** Visualizations of jets with  $J = 8.3$ ,  $M_1 = 2$  and  $M_j$  increasing from 2.1 (Case 7a) to 2.8 (Case 7b) to 3.5 (Cases 7c and 7d). Jet gas is helium for Cases 7a–c, argon for Case 7d

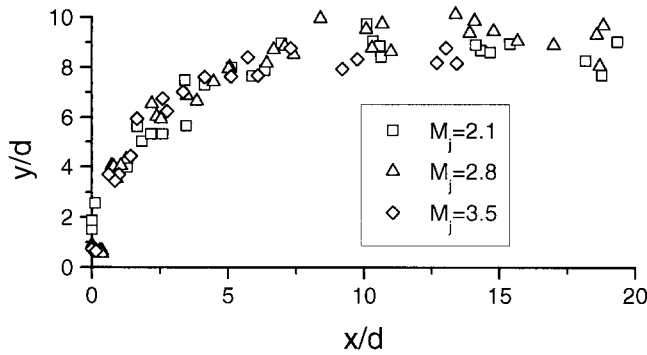


Fig. 4. Trajectories of helium and argon jets with  $J = 8.3$  and  $M_1 = 2$

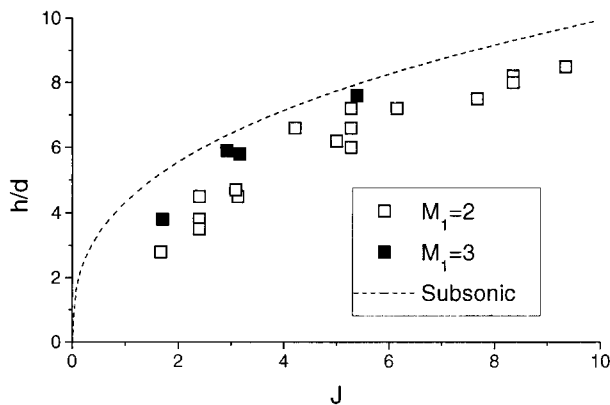


Fig. 5. Penetration versus momentum ratio

jets achieve about the same penetration as pressure-matched jets. The same behavior was observed in the comparisons between cases 1a–b, 3a–b, 3c–d, and 5a–c. Even though, as mentioned earlier, it is hard to distinguish between the effects of  $M_j$  and  $p_j/p_2$  at fixed  $J$ , the present results suggest that both  $M_j$  and  $p_j/p_2$  are not influential on penetration.

Increasing the cross-flow Mach number  $M_1$  from 2 to 3, and keeping  $J$  fixed, produced a slight increase in penetration on the order of one jet diameter. This was noticed in the comparisons between cases 1b–c, 3b–c, and 5c–d. The increased penetration can perhaps be explained by considering the near field of the jet as an inviscid circular cylinder in a cross flow. At supersonic velocities, the drag coefficient of the cylinder declines with Mach number (see Schetz and Billig, 1966, for example). Consequently, at fixed  $J$ , the force causing the jet to bend is less at  $M_1 = 3$  than it is at  $M_1 = 2$ , resulting in better penetration.

Fig. 5 depicts a plot of  $h/d$  versus  $J$  and  $M_1$ . The slight increase in penetration with increasing  $M_1$  is apparent. Although an exact power-law dependence of  $h/d$  on  $J$  is difficult to infer from our data, we attempt here a rough comparison with the subsonic scaling laws. Pratte and Baines (1967) found experimentally that the upper edge of the subsonic

transverse jet  $y(x)$  is described by

$$\frac{y}{rd} = 2.63 \left( \frac{x}{rd} \right)^{0.28}$$

where  $r = U_j/U_1$ . Extending this to variable density, we replace  $r$  by  $\sqrt{J}$  and evaluate at  $x/d = 6$  (the axial location of our penetration measurements) to obtain the equivalent subsonic penetration:

$$\left( \frac{h}{d} \right)_{\text{subsonic}} = 4.34 J^{0.36} \quad (6)$$

The subsonic relation is overlaid in Fig. 5. It is evident that the penetration scaling of the supersonic transverse jet is not dramatically different from that of the subsonic jet.

## 5 Conclusions

Penetration of a supersonic injected normal into a supersonic cross flow depends strongly on the momentum ratio  $J$  and is insensitive to local conditions near the jet exit. Penetration height increases with  $J$  in a fashion similar to that found in subsonic flows. Increasing free-stream Mach number  $M_1$  modestly improves penetration, while the jet Mach number  $M_j$  and density ratio  $\rho_j/\rho_2$  have no noticeable effect. Highly under-expanded jets achieve about the same penetration as pressure-matched jets. The flow is highly unsteady, a feature that may significantly affect mixing and combustion.

## Acknowledgements

This work was supported by AFWAL contract F33615-88-C-2889, with Dr. Abdollah Nejad the contract monitor. We are thankful to Professor G. S. Samuelsen for his supervision of the contract and to Mr. Mike Lin for his assistance with the experiments.

## References

- Abramovich, G. N. 1963: The theory of turbulent jets. Cambridge: MIT Press
- Billig, F. S.; Orth, R. C.; Lasky, M. 1971: A unified analysis of gaseous jet penetration. AIAA J. 9, 1043–1058
- Broadwell, J. E.; Breidenthal, R. E. 1984: Structure and mixing of a transverse jet in incompressible flow. Fluid Mech. 148, 405–412
- Heister, S. D.; Karagozian, A. R. 1990: Gaseous jet in supersonic crossflow. AIAA J. 28, 819–827
- McDaniel, J. C.; Graves, J. 1988: Laser-induced fluorescence visualization of transverse gaseous injection in a nonreacting supersonic combustor. J. Prop. Power 4, pp. 591–597
- Pratte, B. D.; Baines, W. D. 1967: Profiles of the round turbulent jet in a cross flow. J. Hydronaut. Div. ASCE 92, p. 53
- Schetz, J. A.; Billig, F. S. 1966: Penetration of gaseous jet injected into a supersonic stream. J. Spacecraft 3, 1658–1665
- Schetz, J. A.; Weinraub, R. A.; Mahaffey, R. E. 1968: Supersonic transverse injection into a supersonic stream. AIAA J. 6, 933–934
- Zukoski, E. E.; Spaid, F. W. 1964: Secondary injection of cases into a supersonic cross flow. AIAA J. 2, 1689–1996